Axial capacity of reactive powder concrete filled steel tube columns with two load conditions

Qiuwei Wang [*1,2], Qingxuan Shi [1,2a], Zhaodong Xu [2,3a] and Hanxin He [2b]

[1] *State Key Laboratory of Green Building in Western China,*
Xî an University of Architecture and Technology, No. 13 Yanta Road, Xî an, P.R. China
[2] *College of Civil Engineering, Xî an University of Architecture and Technology, No. 13 Yanta Road, Xî an, P.R. China*
[3] *College of Civil Engineering, Southeast University, Sipailou 2#, Nanjing, P.R. China*

Abstract. Reactive powder concrete (RPC) is a type of ultra-high strength concrete that has a relatively high brittleness. However, its ductility can be improved by confinement, and the use of RPC in composite RPC filled steel tube columns has become an important subject of research in recent years. This paper aims to present an experimental study of axial capacity calculation of RPC filled circular steel tube columns. Twenty short columns under axial compression were tested and information on their failure patterns, deformation performance, confinement mechanism and load capacity were presented. The effects of load conditions, diameter-thickness ratio and compressive strength of RPC on the axial behavior were further discussed. The experimental results show that: (1) specimens display drum-shaped failure or shear failure respectively with different confinement coefficients, and the load capacity of most specimens increases after the peak load; (2) the steel tube only provides lateral confinement in the elastic-plastic stage for fully loaded specimens, while the confinement effect from steel tube initials at the set of loading for partially loaded specimens; (3) confinement increases the load capacity of specimens by 3% to 38%, and this increase is more pronounced as the confinement coefficient becomes larger; (4) the residual capacity-to-ultimate capacity ratio is larger than 0.75 for test specimens, thus identifying the composite columns have good ductility. The working mechanism and force model of the composite columns were analyzed, and based on the twin-shear unified strength theory, calculation methods of axial capacity for columns with two load conditions were established.

Keywords: circular composite columns; reactive powder concrete (RPC); load conditions; constraint mechanism; axial capacity

1. Introduction

Reactive powder concrete (RPC) is the new generation of concrete with ultra-high strength, remarkable durability and high toughness. The outstanding mechanical properties achieved are compressive strength, Young's modulus and fracture energy in the range of 200-800 MPa, 50-75 GPa and 12-40 kJ/m^2, respectively (Yiğiter *et al.* 2012, Zheng *et al.* 2015, Sanchayan and Foster 2016, Abid *et al.* 2017, Abdulkareem *et al.* 2018). Owing to these remarkable properties, RPC has been used in diverse engineering fields such as civil, municipal, petroleum and military structures, and its commercial production has also started in many countries with increasing demand. In recent years, there has been more research work on the mix designs and mechanical behavior of RPC, and effects of ingredients, mix proportions and curing methods are the focused areas. The research results indicate that RPC is a brittle material and post-peak brittle failure often occurs when it is subject to high compression level which will limit its application (Li and Liu 2016). Adding steel fibers can improve the tensile ductility of RPC, but they are unable to enhance its compressive ductility (Yan *et al.* 2016). However, both strength and ductility of RPC can be increased when it is under confinement.

A RPC filled steel tube system has been shown to exhibit high load capacity with excellent deformation performance. The axial behavior is a basis to investigate other mechanical properties of RPC filled steel tube columns, but when compared to ordinary concrete - filled steel tube (CFST) columns, research on the behavior of RPC filled steel tube columns under axial compression is not plentiful. For ordinary CFST columns, Han and An (2014) studied the behavior of CFST stub columns under axial compression, and developed a finite element analysis modeling to analyze the axial capacity of the composite columns. Aslani *et al.* (2015) assessed available experimental results on ordinary CFST columns, and developed simplified relationships to predict the ultimate buckling capacities of short columns subjected to concentric loading. Du *et al.* (2017) employed artificial neural network (ANN) models to predict the axial bearing capacity of rectangular CFST columns based on the experimental data, and thought that the effects of parameters on the axial bearing capacity of columns differed from design codes.

∗Corresponding author, Ph.D., Associate Professor,
 E-mail: wqw0815@126.com
[a] Ph. D., Professor
[b] Ph. D., Lecturer

Liang *et al.* (2018) presented a new stiffening method with inclined stiffeners to investigate the behaviors of CFST columns under axial compression, and applied a nonlinear finite element model to simulate the mechanical performances. Other researches who have studied the axial behaviors of CFST columns include Huang *et al.* (2012), Evirgen *et al.* (2014), Choi *et al.* (2017), Chen *et al.* (2018), Thomas and Sandeep (2018). However, constituents used in preparing RPC mixtures are different from the conventional concrete mixtures. Compared with the ordinary concrete, RPC minimizes the internal porosity and microcracks inside the material, obtains high strength and durability by improving the activity of the components. Therefore, the axial load behaviors of composite columns using ordinary concrete and RPC are different.

On the basis of the research achievement on ordinary CFST columns, the scholars have begun to concern the studies on the behavior of RPC filled steel tube columns. Feng (2008) studied the interaction between steel tubes and the RPC core, as well as the influence of interaction on bearing capacity and deformability of RPC filled steel tubular stub columns under axial loads. Min *et al.* (2013) proposed a unified formula to calculate the axial load capacity of CFST columns with circular and polygonal sections. Parametric studies were then conducted to investigate the effect of confinement on RPC strength. Hoang and Fehling (2017) presented a review of past experimental studies to have a deeper insight into the axial compressive behavior of UHPC (Ultra-high performance concrete) filled steel tube columns, and investigated the influence of the confinement index on the load capacity of composite columns. Luo *et al.* (2017) carried out axial

compressive tests of RPC-filled steel tube columns, and presented a stress-strain model for RPC confined by steel tube, and others (Guler *et al.* 2013, Huynh *et al.* 2015, Shi *et al.* 2017, Shan *et al.* 2018). In the previous studies, the axial load was always applied to both the steel tube and the RPC core. When the steel tube yields, the confinement effect is reduced and the load capacity of the composite column cannot be fully realized. In addition, because high temperature curing was not very practical for cast-in-situ structures, the RPC core used in these studies was often cured under normal temperature, which tends to limit the full capacity of this special type of concrete.

The work presented in this paper is an extension of research on RPC conducted by the first author (Wang *et al.* 2017). Twenty specimens with two mix designs, two curing temperatures (normal and high), two load conditions (full and partial), and four steel tube diameter-to-thickness ratios were tested in the study. Test results were evaluated in terms of failure patterns, load-deformation curves, steel tube strains and load capacity. The working mechanism and force model of short columns were analyzed, and based on the twin-shear unified strength theory, calculation methods of axial capacity for RPC filled steel tube columns with two load conditions were then proposed.

2. Experimental program

2.1 Specimens design and preparation

The test presented in this study consisted of twenty RPC filled circular steel tube columns. To preclude buckling, the

Table 1 Main parameters of specimens

Specimens	$D \times t \times L$ (mm³)	Curing systems	Loading conditions	f_{cu} (MPa)	f_y (MPa)	ξ	D/t	A_s/A_c
AR4.5-1	133×4.5×400	90℃	fully loaded	160	300	0.35	29.56	15%
BR4.5-1	133×4.5×400	90℃	partially loaded	160	300	0.35	29.56	15%
AR4.5-2	133×4.5×400	90℃	fully loaded	140	300	0.40	29.56	15%
AR6.0-1	133×6.0×400	90℃	fully loaded	160	300	0.49	22.17	21%
BR6.0-1	133×6.0×400	90℃	partially loaded	160	300	0.49	22.17	21%
AR6.0-2	133×6.0×400	90℃	fully loaded	140	300	0.56	22.17	21%
AR8.0-1	133×8.0×400	90℃	fully loaded	160	300	0.68	16.63	29%
BR8.0-1	133×8.0×400	90℃	partially loaded	160	300	0.68	16.63	29%
AR8.0-2	133×8.0×400	90℃	fully loaded	140	300	0.78	16.63	29%
AR10.0-1	133×10.0×400	90℃	fully loaded	160	300	0.90	13.30	39%
BR10.0-1	133×10.0×400	90℃	partially loaded	160	300	0.90	13.30	39%
AR10.0-2	133×10.0×400	90℃	fully loaded	140	300	1.03	13.30	39%
AZ4.5-1	133×4.5×400	normal	fully loaded	120	300	0.56	29.56	15%
BZ4.5-1	133×4.5×400	normal	partially loaded	120	300	0.56	29.56	15%
AZ6.0-1	133×6.0×400	normal	fully loaded	120	300	0.78	22.17	21%
BZ6.0-1	133×6.0×400	normal	partially loaded	120	300	0.78	22.17	21%
AZ8.0-1	133×8.0×400	normal	fully loaded	120	300	1.10	16.63	29%
BZ8.0-1	133×8.0×400	normal	partially loaded	120	300	1.10	16.63	29%
AZ10.0-1	133×10.0×400	normal	fully loaded	120	300	1.44	13.30	39%
BZ10.0-1	133×10.0×400	normal	partially loaded	120	300	1.44	13.30	39%

height-to-diameter ratio of all the specimens was set at 3.0. The criterion to design the test parameters is to consider as many parameters as possible within the limited specimens. The main parameters included in the present study were load conditions, curing temperatures, diameter-to-thickness ratio of the steel tubes and compressive strength of RPC. Two different methods were used to apply the axial load on the specimens. If the load is applied to the entire cross-section, the specimen is said to be fully loaded; and if the load is applied only on the RPC core, the specimen is said to be partially loaded. In the fully loaded case, both the steel tube and the RPC core are under direct axial stress, but in the partially loaded case, only the RPC core is subjected to a directly axial stress. To study the effect of curing temperature on RPC strength, two curing temperatures (high temperature of 90°C and normal temperature that corresponds to 15-20°C) were used. In addition, the external diameter of all the steel tubes was 133 mm, but the wall thickness of 4.5 mm, 6.0 mm, 8.0 mm and 10.0 mm were used. Three target (or design) cube compressive strengths for RPC-160 MPa, 140 MPa and 120 MP - were used in the test. A summary of major parameters used in the present study is given in Table 1.

The nomenclature used in Table 1 is as follows: the letters A and B denote fully and partially loaded specimens, respectively. The letters R and Z represent curing temperatures of 90°C and normal, respectively. The numbers 4.5, 6.0, 8.0 and 10.0 refer to the thicknesses of the steel tube. The numbers 1 and 2 designate the two RPC mix designs shown in Table 2. The variables D, t and L denote the external diameter, thickness and height of the steel tube, respectively; f_{cu} and f_y are the measured cube strength of RPC and the yield strength of the steel tube; and A_s and A_c are the cross sectional area of the steel tube and RPC core. The symbol ξ is the confinement coefficient, defined as the ratio of the axial capacity of the steel tube to the RPC core, and given by the expression of $A_s f_y / A_c f_c$, where f_c is the compressive strength of rectangular prism shaped RPC specimens. A larger value for ξ indicates a stronger lateral confinement provided by steel tube.

The ingredients used for RPC included P. O. 42.5 ordinary Portland cement (Chinese standard GB 175-2007), silica fume, quartz powder, silica sand, steel fiber, super-plasticizer and water. They were all purchased locally. The proportions and fineness of the ingredients were determined using dense packing theory to minimize internal defects such as voids and microcracks so optimal performance for the RPC can be achieved. Two design mixes with different steel fiber content as shown in Table 2 were used.

The RPC ingredients were mixed in a high-speed mixer and manually compacted using standard vibrators. Each test specimen was fabricated using the following procedure: The steel tube was secured in a wooden mold (Fig. 1(a)) and its bottom was sealed with a mica sheet to prevent concrete from leaking. Freshly mixed RPC was placed in the hollow steel tube in four equal layers and compacted by a vibration rod. An additional layer of RPC was cast on top of the specimen and flattened until no bubbles were present. The specimen was then covered with a plastic film at both ends and was left to cure under room temperature for 24 hours. Thereafter, it was either placed in a 90°C hot water bath (Fig. 1(b)) for the next 72 hours or left to cure under normal temperature for an additional 28 days (Chinese specification GB/T 31387-2015) before the test (Fig. 1(c)).

2.2 Material properties

The cube and rectangular prism specimens with dimensions of 100 mm × 100 mm × 100 mm and 100 mm × 100 mm × 300 mm were prepared to determine the compressive strength of RPC according to Chinese specification GB/T 31387 (Design code 2015). Three groups labeled R1, R2 and Z1 that correspond to mix design 1 using 90°C curing temperature, mix design 2 using 90°C curing temperature and mix design 1 using normal curing temperature were tested by electrohydraulic testing machine. Three specimens were prepared and tested for each group. All specimens were tested to failure and the maximum compressive capacity was recorded. The average compressive strength of the three specimens is shown in

Table 2 RPC mix designs (kg/m³)

Mix design	Components							
	Cement	Silica fume	Quartz powder	Coarse sand	Medium sand	Fine sand	Steel fiber	Super-plasticizer
1	674	169	216	673	313	219	200	21.2
2	674	169	216	673	313	219	120	21.2

(a) The wooden mold (b) 90°C hot water bath (c) Specimens before test

Fig. 1 Fabrication of specimens

Table 3 Compressive strength of RPC

Groups	Mix design	Curing temperature	Cube strength f_{cu} (MPa)	Rectangular prism strength f_c (MPa)
R1	1	90°C	151.6	120.5
R2	2	90°C	128.8	108.2
Z1	1	normal	127.1	106.6

Table 3. It can be seen that the prism strengths are lower than the cube strengths. And, the measured RPC cube strengths for groups R1, R2 and Z1 are 5% and 8% lower, and 6% higher than their respective designed values. Although these percent errors are considered well within the design limit, the measured compressive strength should be used to analyze the axial-load behavior of specimens. The specimens R2 and Z1 were mixed at different time due to the holiday, and the steel fibers used for R2 and Z1 were various batches from the same manufacturing company. The slight difference in mixing time and ingredient is maybe the main reason which leads to the quite closer strength values of R2 and Z1.

To determine the mechanical properties of steel, three standard tension specimens with four different thicknesses were made and tested. The yield strength, tensile (or ultimate) strength and elastic modulus were measured using an electronic universal testing machine and extensometers. The results are shown in Table 4.

2.3 Test setup and loading history

Tests were performed using a 5000-kN capacity TYA-2000 universal testing machine, and test setups for the fully and partially loaded specimens are shown in Fig. 2. For fully loaded specimens, the steel tube and RPC were subjected to the axial load together through the upper and lower bearing plates. However, steel pads with a diameter of 3 mm smaller than the internal diameter of the steel tube were placed at two ends of partially loaded specimens, so that the axial load was directly applied only to the RPC core. All specimens were tested according to automatic two-stage control mode. Columns were tested in a load-controlled manner at a loading rate of about 5 kN/s until 90% of the pre-estimated peak load was reached. Then displacement control was used at approximately 0.1 mm/min until the specimen failed. The test was stopped when the local crippling of steel tube or large axial deformation of the specimen was observed.

2.4 Instrumentation

During the test, the axial load, specimen deformation and strains of the steel tube and RPC core were measured and recorded automatically. The axial load was measured by the sensor installed on the actuator, and the axial displacement was measured using four linear variable displacement transducers (LVDTs) that were mounted onto the four sides of specimens, attached to the middle region of the column (Fig. 3). Strain gauges were spaced 100 mm longitudinally along the specimen height and bonded onto
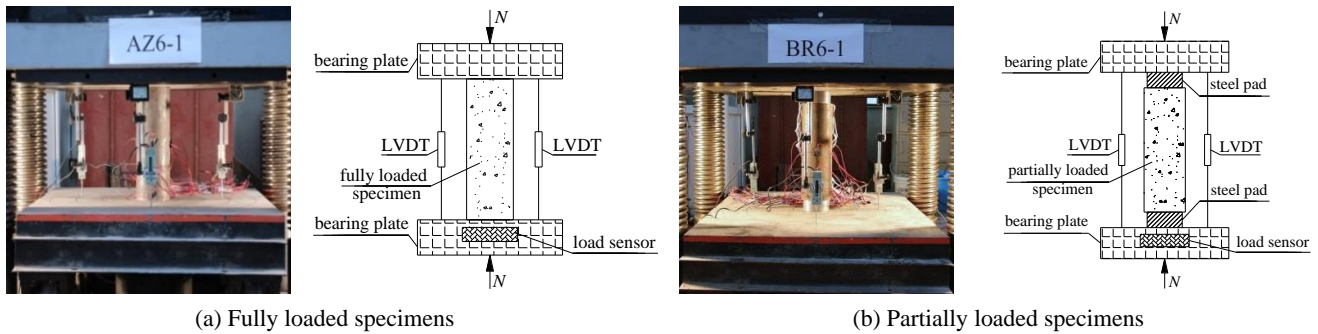

(a) Fully loaded specimens

(b) Partially loaded specimens

Fig. 2 Test setup

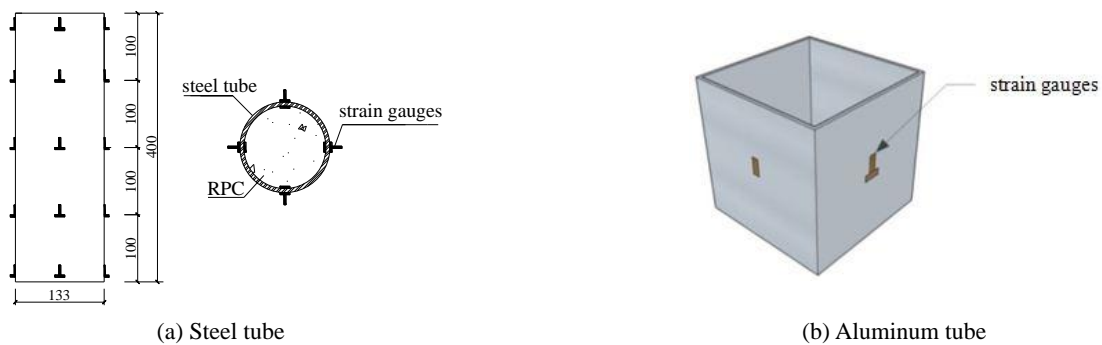(a) Steel tube

(b) Aluminum tube

Fig. 3 Instrumentation

the surface of the steel tube in both axial and transverse directions. At each level, four measuring points around the perimeter of cross section were used. An additional four transverse strain gauges were placed on the inside surface of steel tube at mid-height of the specimen before the RPC was cast. The locations of strain gauges are shown schematically in Fig. 3(a).

Besides this, to measure the strain at the center of the RPC core, a rectangular aluminum tube with dimensions of 40 mm × 40 mm × 40 mm that has elastic modulus (6.9 × 10^9 MPa) and compressive strength (145 MPa) comparable to those of RPC was placed into partially loaded specimens. Although there are slight differences between these values, this difference has no obvious effect on the collaborate work of aluminum tube and RPC. Axial and transverse strain gauges were adhered to four sides of the aluminum tube covered with heat-resistant epoxy resins (Fig. 3(b)). The box was placed into the inner RPC during casting, and two U-shaped slots were set at two ends of steel tube through which the leads can be channeled. All measurements were monitored by an electronic data acquisition system that simultaneously recorded all data at intervals of 0.5 s.

3. General behavior and failure pattern

The final failure modes for all specimens are shown in Fig. 4. The failure mechanism of fully and partially loaded specimens is different, described as follows.

There was no damage for the fully loaded specimens before 80% of the load capacity was reached. After that, local crippling started to occur in the steel tube, and central points of upper and lower cross sections deviated from the longitudinal axis of specimens with the increasing load. Local crippling of steel tube is like a drum and could be called drum-shaped failure. The drum-shaped failure is more obvious for specimens AR10.0-1, AR10.0-2 and AZ10.0-1 with large confinement coefficient, for which the steel tube could provide stronger lateral confinement to inner concrete. Other specimens display a combination of drum-shaped failure and shear failure: the shear failure

surface extended from the top to the bottom for specimens AR4.5-1 and AR4.5-2, while only extended from the top to middle part for specimens AR8.0-1 and AR8.0-2. And for the specimens AR6.0-1 and AR6.0-2 with medium confinement coefficient, the range of failure surface was about 3/4 of the column height. Thus a smaller confinement coefficient would lead to more obvious shear failure. The partially loaded specimens display shear failure except the specimen BZ10.0-1, and the reason is that the lateral confinement provided by the steel tube has a significant impact on the failure modes of specimens. Just as the specimens AR10.0-1, AR10.0-2 and AZ10.0-1, the specimen BZ10.0-1 displays drum-shaped failure because of its large confinement coefficient. For other partially loaded specimens (except BZ10.0-1), inclined slip lines appeared on the surface of the specimens when approximately 90% of the axial load capacity was attained. Upon reaching the load capacity of the specimen, the RPC core started to crack and deformation was accelerated. At this point, visible distortions were observed on the side of steel tube when the RPC core underwent shear failure. A larger diameter-to-thickness ratio leads to a smaller confinement coefficient, and thus the more obvious distortion would be shown at ends of the steel tube.

4. Experimental results and discussion

4.1 Axial load-strain curves

The axial load (N) - strain (ε) curves and the corresponding normalized curves (N/N_0-$\varepsilon/\varepsilon_0$) are shown in Fig. 5. Where axial strain ε is defined as the ratio of axial deformation l to the height of specimen L, and N_0 and ε_0 are the peak load and peak stain respectively. The dot on each N-ε curve marks the load that is denoted as the axial load capacity N_{ue}. Although the axial loads for some specimens continue to increase after the dot, this increase is accompanied by relatively large axial deformation, and are discarded for design purpose. Two observations can be drawn from these N-ε curves:

| AR4.5-1 | AR6.0-1 | AR8.0-1 | AR10.0-1 | AR4.5-2 | AR6.0-2 | AR8.0-2 | AR10.0-2 | AZ4.5-1 | AZ6.0-1 |

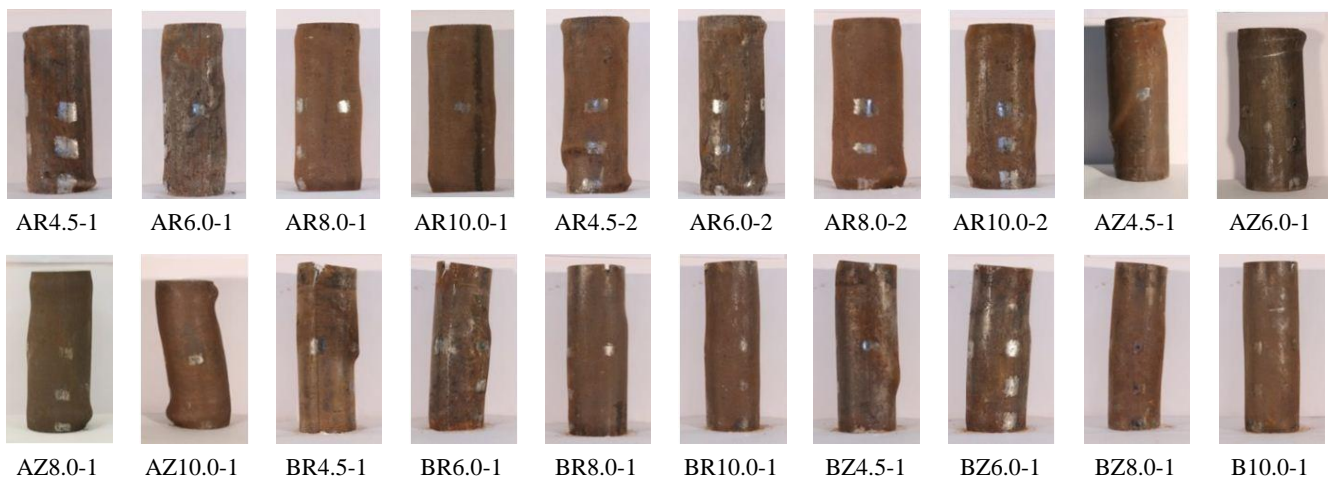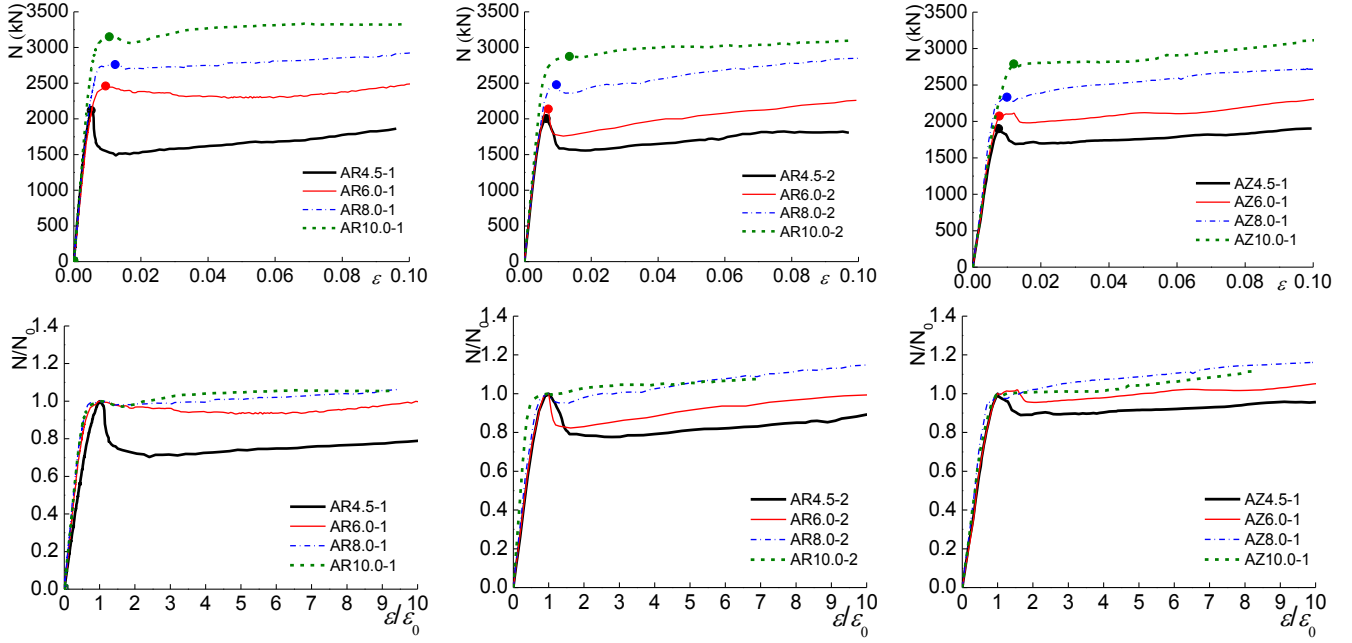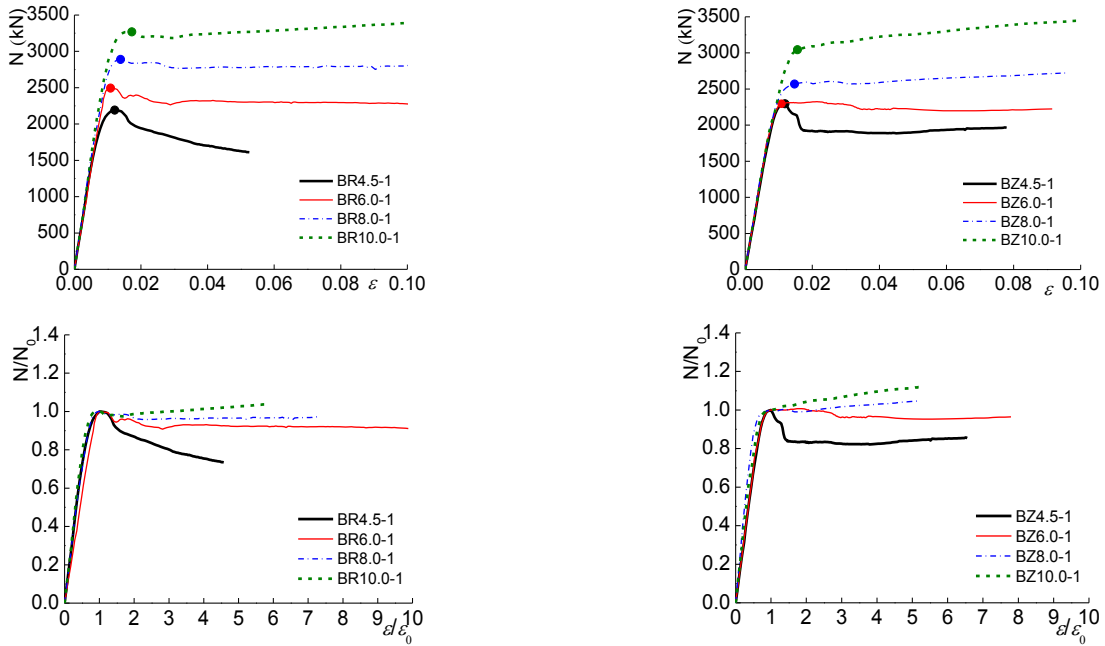| AZ8.0-1 | AZ10.0-1 | BR4.5-1 | BR6.0-1 | BR8.0-1 | BR10.0-1 | BZ4.5-1 | BZ6.0-1 | BZ8.0-1 | B10.0-1 |

Fig. 4 Failure modes of specimens

(a) Fully loaded specimens

(b) Partially loaded specimens

Fig. 5 Axial load-strain curves

(1) There is a linear relationship between axial load and strain in the initial stage. The curve begins to be nonlinear when the applied load reaches 60% to 80% of N_{ue}, and then different phenomenon will be presented for specimens with different parameters: for specimens with relatively thin steel tubes (4.5 mm and 6.0 mm), there is a sudden drop after N_{ue} followed by no or a slight increase in N as the strain increases; for specimens with thick steel tubes (8.0 mm and 10.0 mm), there is no or only a slight drop in load after N_{ue} followed by a gradual increase as the strain increases. A thicker steel tube

could lead to a stronger lateral confinement, and thus contributing to a higher axial load capacity for the specimens.

(2) The load capacity N_{ue} of partially loaded specimens is much higher than that of fully loaded specimens (see Table 5). The reason is that no direct axial stress is induced in steel tubes for partially loaded specimens, and so more efficient confinement could be provided to the inner RPC. Meanwhile, the specimens have higher axial capacity with larger steel tube thickness and compressive strength of RPC, and the ductility is more pronounced for
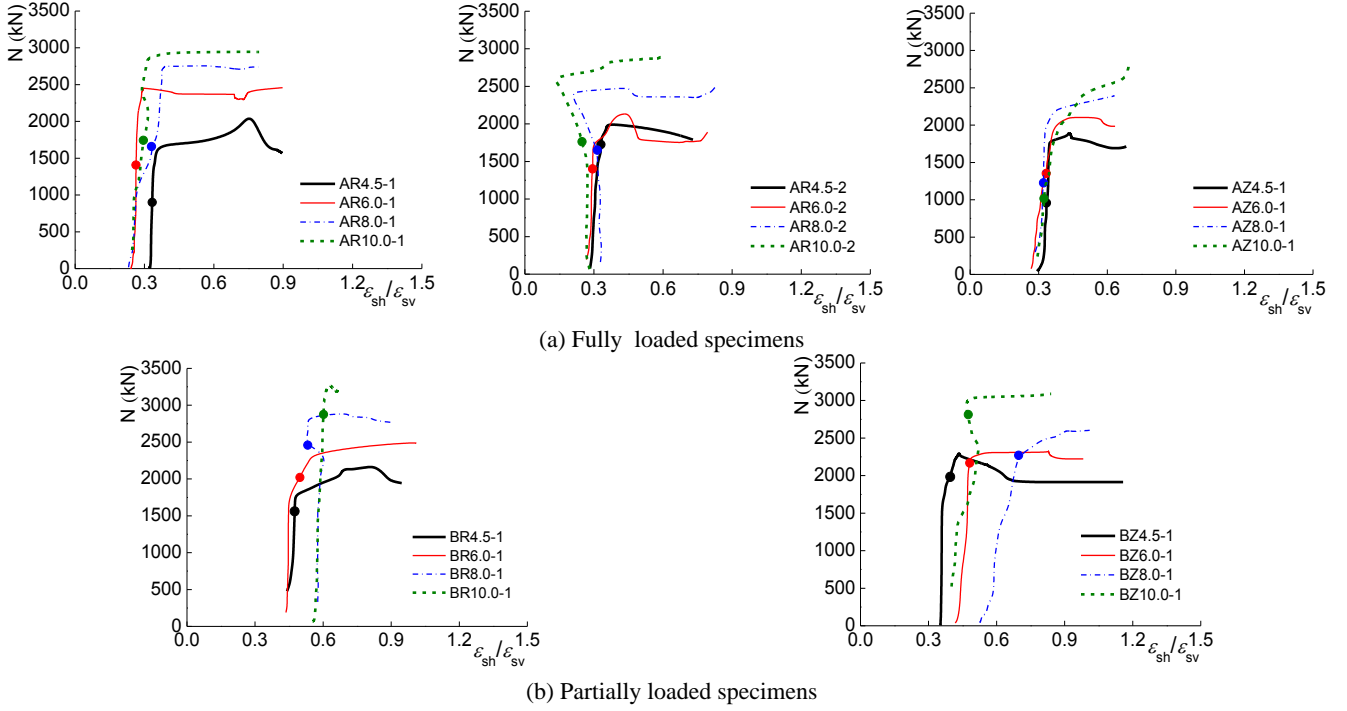
(a) Fully loaded specimens

(b) Partially loaded specimens

Fig. 6 Transverse to longitudinal strain ratio of steel tube

specimens with larger confinement coefficients.

4.2 The strain of steel tube

The strain of steel tube is an evidence of its constraints on RPC core, and the ratio of transverse strain ε_{sh} to longitudinal strain ε_{sv} can reflect the deformation of steel tube along two directions. Fig. 6 shows the relation between axial load N and the ratio $\varepsilon_{sh}/\varepsilon_{sv}$ for specimens, where the dot denotes the yield point for steel tube. The radial stress of the steel tube is only 5% of the axial stress, and so the radial stress will be ignored in the analysis. It can be seen from the figure that:

(1) The transverse to longitudinal strain ratio $\varepsilon_{sh}/\varepsilon_{sv}$ keeps stable at the early loading stage. The ratio becomes larger after the steel tube yields and increases rapidly after N_{ue}. The ratio is larger than 0.6 at the ultimate state for most specimens, which is greater than the Poisson's ratio (about 0.3) of steel tube. So the confinement effect is not obvious at the beginning and mainly initiates at the elastic-plastic stage.

(2) On the average, the ratio $\varepsilon_{sh}/\varepsilon_{sv}$ for partially and fully loaded specimens is 0.5-0.6 and 0.3 respectively at the yield point of steel tube. This indicates that there is no interaction between steel tube and RPC at early stage for fully loaded specimens, while the steel tube could provide lateral confinement to RPC core at the onset of loading for partially loaded specimens.

(3) The longitudinal strain is larger than transverse strain for partially loaded specimens, thus identifying that although no direct axial load is applied, the steel tube could still bear the axial

compression through the interaction friction. The maximum ratio $\varepsilon_{sh}/\varepsilon_{sv}$ before yielding is larger for the partially loaded specimens, from which it can be concluded that the steel tube could provide larger confinement without bearing direct axial load.

4.3 Axial capacity

4.3.1 Ultimate capacity

The measured ultimate capacity N_{ue} of specimens is presented in Table 5. The term N_{s+c} (defined as $A_c f_c + A_s f_y$) represents the load capacity without taking into consideration the effect of confinement provided by the steel tube, that is, N_{s+c} is simply the superposition of load capacities of the RPC core and steel tube. It can be seen that the ratio N_{ue} to N_{s+c} for all specimens is larger than 1.0, indicating the ultimate capacity of the composite specimen is higher than that of the sum of the load capacities of its individual constituents, thus reflecting the beneficial effect of confinement. Meanwhile, the mean values of N_{ue}/N_{s+c} for fully and partially specimens are 1.12 and 1.24 respectively. The main reason is that buckling of the steel tube could be avoided at the ultimate state when only applied to RPC core, which enables the steel tube to provide more effective confinement, consequently improving the ultimate capacity and ductility of composite columns.
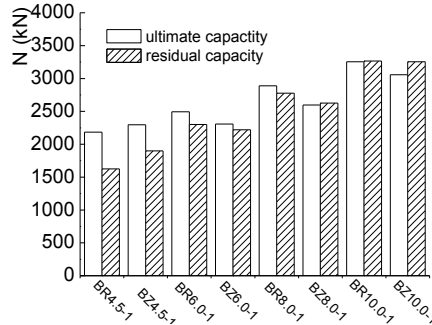
A smaller diameter-to-thickness ratio (D/t) will lead to a larger confinement coefficient under other same conditions, and the variations of the ultimate capacity with diameter-to-thickness ratios for all test specimens are plotted in Fig. 7. Where AR-1, AR-2, AZ, BR and BZ denote different series of specimens and four specimens are included in each series. As can be seen from the figure that, the ultimate capacity increases with the decrease of diameter-to

Table 5 Ultimate capacity of specimens

Specimen	AR4.5-1	BR4.5-1	AR4.5-2	AR6.0-1	BR6.0-1	AR6.0-2	AR8.0 -1	BR8.0 -1	AR8.0 -2	AR10.0-1
N_{ue} (kN)	2119	2184	2004	246.00	2494	2137	2758	2889	2478	3150
N_{s+c} (kN)	2055	2066	1906	2147	2157	2006	2317	2326	2184	2414
N_{ue}/N_{s+c}	1.03	1.06	1.05	1.15	1.16	1.07	1.19	1.24	1.13	1.30
Specimen	BR10.0-1	AR10.0-2	AZ4.5-1	BZ4.5-1	AZ6.0-1	BZ6.0-1	AZ8.0 -1	BZ8.0 -1	AZ10.0-1	BZ10.0-1
N_{ue} (kN)	3255	2711	1900	2296	2113	2307	2334	2597	2789	3057
N_{s+c} (kN)	2423	2291	1887	1811	1987	1915	2167	2099	2275	2212
N_{ue}/N_{s+c}	1.34	1.18	1.01	1.27	1.06	1.21	1.08	1.24	1.23	1.38
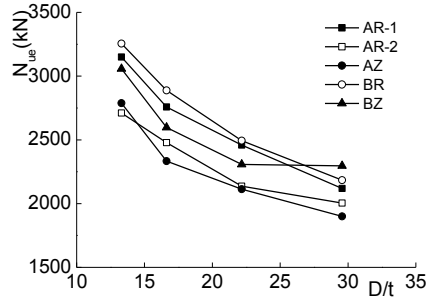
(a) N_{ue}-D/t curves
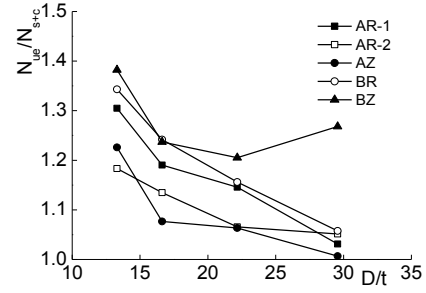
(b) N_{ue}/N_{s+c}-D/t curves

Fig. 7 The effect of D/t on ultimate capacity
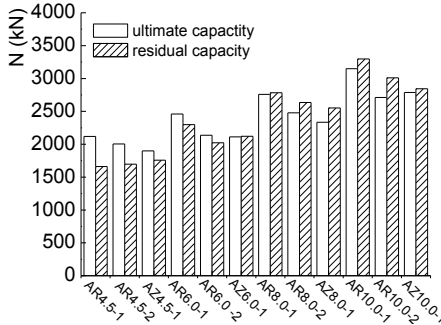
(a) Fully loaded specimens

(b) Partially loaded specimens
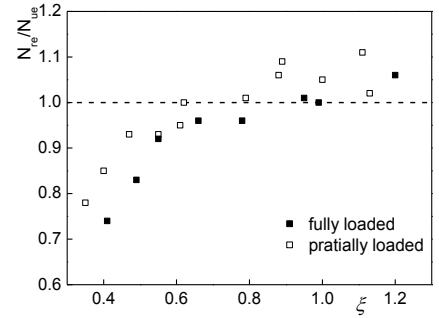
(c) N_{re}/N_{ue} vs ξ

Fig. 8 The comparison of N_{ue} and N_{re}

thickness ratios. However, their relationship is not linear, and the increase of ultimate capacity will be more significant with a smaller diameter-to-thickness ratio. Moreover, the ratio N_{ue}/N_{s+c} also increases with the decrease of D/t, although the changing rules are different for all specimens, the analysis still indicates that a smaller ratio D/t will contribute more axial load capacity to specimens and the composite effect would be obvious.

4.3.2 Residual capacity

The residual capacity N_{re} means the capacity that composite columns could have after failure. The residual capacity is defined as the load capacity when the axial strain ε is 0.05 according to the test result. The reason is that test specimens will have relatively large axial deformation at this point ($\varepsilon = 0.05$), although there is no descending part for N-ε curves of most specimens. The comparison of

ultimate capacity N_{ue} and residual capacity N_{re} is shown in Figs. 8(a)-(b), and the variation of the ratio N_{re}/N_{ue} with the confinement coefficient is plotted in Fig. 8(c).

It can be seen that the confinement effect provided by the steel tube could improve the ductility, and so the specimens still have higher load capacity after their failure. Meanwhile, the residual capacity and the ratio N_{re}/N_{ue} for partially loaded specimens are larger than that of fully loaded specimens, and both N_{re} and N_{re}/N_{ue} increase as the confinement coefficient ξ increases. These observations indicate that the residual capacity and confinement effect are more pronounced for a thicker steel tube which is not subjected to any direct load. In addition, the property of steel tube after yield also has an impact on the residual capacity, manifested as that the N_{re} will be higher with a larger hardening modulus.

5. Calculation methods for the axial capacity

5.1 The current calculation method

The calculation theories for the axial capacity of CFST columns mainly include the unified strength theory, the limit equilibrium theory and others. A variety of calculation formulas for axial capacity has been proposed based on these methods. For fully loaded RPC filled steel tube columns, there have been some calculation methods obtained from experimental studies and numerical simulations, and the common uses are as follows.

Zhang (2003) measured the load capacity of RPC filled steel tube columns under axial compression, and put forward Eq. (1) by fitting the test data

$$N_\mathrm{u} = A_\mathrm{c} f_\mathrm{c}(1+1.2\xi) \tag{1}$$

Lin *et al.* (2005) analyzed the test results of 39 RPC filled steel tube columns, and proposed the simplified calculation formula (Eq. (2)) of axial capacity which considered the contributions of steel tube and confined RPC

$$N_\mathrm{u} = f_\mathrm{y} A_\mathrm{s} + f_\mathrm{co} A_\mathrm{c} \tag{2}$$

Where f_co is the uniaxial compressive strength of confined RPC, determined as $f_\mathrm{co} = f_\mathrm{c}[1.2 + 0.25(100/f_\mathrm{c})^{1.25}\zeta^2 - 0.04\xi]$.

Feng (2008) presented the simplified calculation method (Eq. (3)) for RPC filled steel tube short columns based on

specifications of different countries. For safety and operation convenience, the coefficient k was set as 1.0

$$N_\mathrm{u} = f_\mathrm{c} A_\mathrm{c} + k f_\mathrm{s} A_\mathrm{s} \tag{3}$$

Luo *et al.* (2014) also proposed the practical calculation methods for RPC filled steel tube columns under axial loads using the limit equilibrium theory, as shown in Eq. (4)

$$N_\mathrm{u} = A_\mathrm{c} f_\mathrm{c}(1+1.188\xi) \tag{4}$$

The above formulas have been used to calculate 94 test specimens from the literatures (Zhang 2003, Lin *et al.* 2005, Feng 2008 and Luo *et al.* 2014) and 12 fully loaded specimens of this article, the calculated results N_ua were compared with the test data N_ue, as shown in Fig. 9. The mean and variance of $N_\mathrm{ua}/N_\mathrm{ue}$ are 0.89 and 1.3% respectively. As can be seen, there is a predictive error between calculated and test results when adopting Eqs. (1)-(4). In addition, it is widely considered that the calculation methods for fully and partially loaded specimens are the same. However, the test result indicates that the stress state and mechanical mechanism of specimens with two load conditions are different, so it is not rational to calculate the axial capacity using the same method.

5.2 The mechanical model

For the fully loaded specimens, the deformation coefficient ($\varepsilon_\mathrm{sh}/\varepsilon_\mathrm{sv}$) of steel tube is smaller than its Poisson's ratio at the initial of loading, and there is no interaction

(a) Eq. (1)
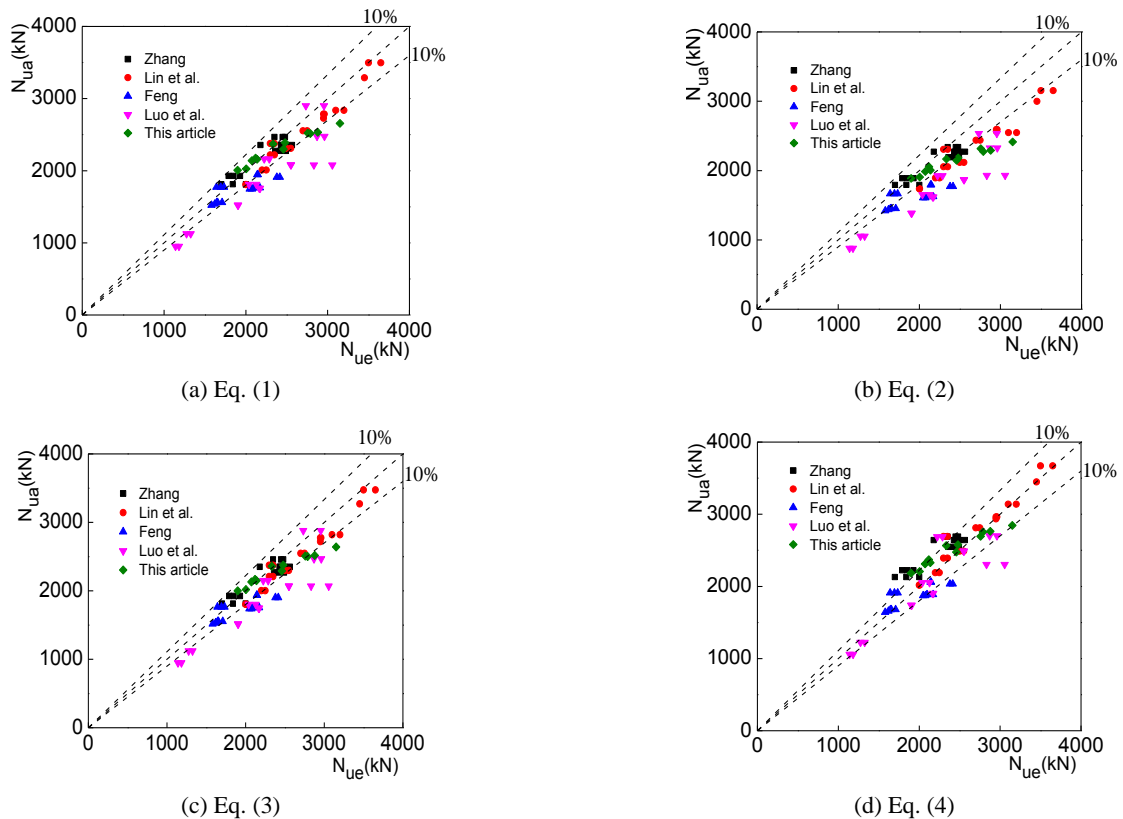

(b) Eq. (2)

(c) Eq. (3)

(d) Eq. (4)

Fig. 9 The calculated results using Eqs. (1)-(4)

between them although the load is applied to the entire cross-section. The interaction force gradually emerges between the steel tube and RPC core with the increasing load. When at higher stress state, the lateral expansion and radial deformation of RPC will be larger than that of steel tube, and the transverse stress of specimens continues to increase so that the redistribution of internal force emerges between steel tube and RPC core. Because of these, the steel tube is thus at the stress state of axial compression, transverse tension and radial compression. For the partially loaded specimens, the deformation coefficient of steel tube is larger than the Poisson's ratio, signifying the confinement effect initiates at an earlier load stage although only the RPC core is subjected to a directly axial stress. The confinement effect will increase as the load increases, and in fact the steel tube also bears certain axial load because of the interface friction, which leads the steel tube to be in a stress state of transverse tension and radial compression. Whatever the load conditions are, the mechanical models of steel tube and RPC core are shown in Fig. 10(a), and the relation between lateral restraint force p and transverse stress σ_θ is presented in Fig. 10(b).

The calculation assumptions including boundary conditions will be adopted during the analysis, as follows: (1) The bond performance between the steel tube and inner RPC is considered to be good, and the contact friction along main directions will be ignored for convenience. (2) The RPC core is in a three-dimensional pressure state, and the tensile strength of RPC is under no consideration after its cracking. (3) The axial deformation of the steel tube and RPC is basically consistent, and the calculation will be based on the equilibrium and deflection compatibility conditions. (4) The upper and lower bearing plates are fit

tightly with the ends of specimens, so that they could be regarded as fixed supports at two ends.

5.3 The proposed calculation method

5.3.1 The fully loaded specimens

The axial load is applied to the steel tube and RPC core together, and so the axial capacity N_u could be expressed as $(N_s + N_c)$, where N_s and N_c are the load capacities of the steel tube and the confined RPC respectively. As can be seen from the section 4.2 that, the steel tube has yielded at the ultimate state and its axial capacity is smaller than $A_s f_y$. The coefficient λ ($\lambda < 1.0$) has been adopted and the axial capacity of the steel tube is defined as $\lambda A_s f_y$. The compressive strength of RPC is denoted as f_{co} and so the load capacity of RPC core could be given by $f_{co} A_c$. Thus, the axial capacity of RPC filled steel tube columns is presented as

$$N_u = \lambda f_y A_s + f_{co} A_c \tag{5}$$

The RPC core is under three-dimensional stress state because of the confinement provided by the steel tube. The principal stresses of RPC in three directions are σ_1, σ_2 and σ_3 respectively and their relation conforms to be $0 > \sigma_1 = \sigma_2 > \sigma_3$. Based on the twin-shear unified strength theory, the axial stress of RPC core can be calculated as

$$-\sigma_3 = f_c - k\sigma_1 \tag{6}$$

The compression and tension are always defined as plus and negative signs, and thus
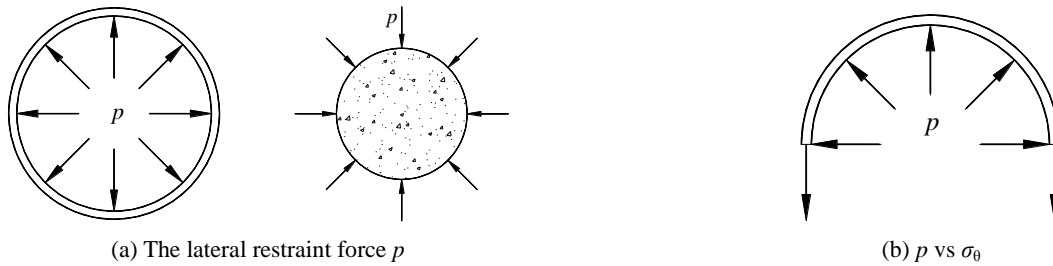
$$\sigma_3 = f_c + k_1\sigma_1 \tag{7}$$

(a) The lateral restraint force p (b) p vs σ_θ

Fig. 10 The mechanical model

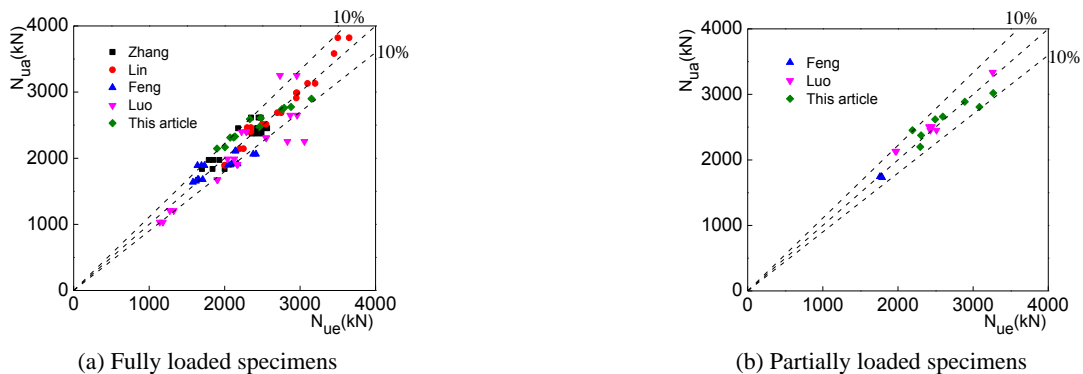(a) Fully loaded specimens   (b) Partially loaded specimens

Fig. 11 The comparison between calculated and test results

Where σ_3 is the compressive strength of confined RPC ($\sigma_3 = f_{co}$). f_c is the uniaxial compressive strength of RPC. k_1 is the strength coefficient and σ_1 is the lateral restraint force p. So, the Eq. (7) could be changed to be Eq. (8)

$$f_{co} = f_c + k_1 p \qquad (8)$$

The steel tube can be regarded as a cylinder which is subjected to axial compression and uniform internal pressure. The test result shows that the relation of the axial stress σ_z, transverse stress σ_θ and radial stress σ_r for steel tube is $\sigma_\theta \geq 0 \geq \sigma_r \geq \sigma_z$, and σ_r is larger than $(\sigma_\theta + \alpha\sigma_z)/(1+\alpha)$. The Eq. (9) can be concluded according to this theory

$$\frac{1}{1+b}(\sigma_\theta + b\sigma_r) - \alpha\sigma_z = \sigma_t \qquad (9)$$

And then

$$\sigma_\theta = (1+b)(\sigma_t + \alpha\sigma_z) - b\sigma_r \qquad (10)$$

Where α is the tension-compression strength ratio of the material, and could be set as 1.0 for steel. σ_t is the tensile yield strength of steel. b is a coefficient reflecting the intermediate main stress, with expression of Eq. (11)

$$b = \frac{(1+\alpha)\tau_s - \sigma_t}{\sigma_t - \tau_s} \qquad (11)$$

Where τ_s is the shear yield strength of steel and the value is $58\sigma_t$. So the coefficient b is 0.38 by substituting $\tau_s = 0.58\sigma_t$ into the Eq. (11).

For a cylinder with radius r, the differential equation with spatial symmetry involving the radial stress σ_r is given by the Eq. (12)

$$r\frac{\partial\sigma_r}{\partial r} + \sigma_r - \sigma_\theta = 0 \qquad (12)$$

By substituting the Eq. (10) to Eq. (12), we can get

$$r\frac{d\sigma_r}{dr} + (1+b)\sigma_r = (1+b)(\sigma_t + \alpha\sigma_z) \qquad (13)$$

The radial stress σ_r can be calculated from the Eq. (13)

$$\sigma_r = (\sigma_t + \alpha\sigma_z) + cr^{-(1+b)} \qquad (14)$$

Suppose that r_0 and r_1 are respectively the internal and external diameters of steel tube. The radial stress σ_r is just $-p$ when the radius $r = r_0$. Then the constant c can be obtained from Eq. (14)

$$c = -[p + (\sigma_t + \alpha\sigma_z)]r_0^{1+b} \qquad (15)$$

By combining the Eq. (14) with the Eq. (15), the expression of σ_r can be written as

$$\sigma_r = (\sigma_t + \alpha\sigma_z)[1 - (\frac{r_0}{r})^{1+b}] - p(\frac{r_0}{r})^{1+b} \qquad (16)$$

The radial stress σ_r will be 0 when the radius $r = r_1$. The Eq. (16) then could be solved with this condition, and the plastic limit solution for lateral constraint p is as follows

$$p = \frac{A_s f_y + \alpha N_s}{A_s}((\frac{r_1}{r_0})^{1+b} - 1) = \frac{A_s f_y + N_s}{A_s}((\frac{r_1}{r_0})^{1.38} - 1) \qquad (17)$$

From above analysis, the axial capacity for fully loaded specimens can be proposed as

$$N_u = [f_c + k_1 f_y(1+\lambda)((\frac{r_1}{r_0})^{1.38} - 1)]A_c + \lambda A_s f_y \qquad (18)$$

Where k_1 and λ are unknown coefficients. Using the nonlinear curve-fitting toolkit in Mathematica, the two coefficients were determined to be $k_1 = 1.11$ and $\lambda = 0.40$ with a mean R^2 value of 0.99 based on the test data of this article. Thus, the Eq. (18) could be further expressed as

$$N_u = [f_c + 1.532 f_y((\frac{r_1}{r_0})^{1.38} - 1)]A_c + 0.4 A_s f_y \qquad (19)$$

5.3.2 The partially loaded specimens

The axial load is applied only to the RPC core but not the entire cross-section, so the axial capacity for partially loaded specimens can be presented as

$$N_u = f'_{co} A_c \qquad (20)$$

In which the symbol f'_{co} is adopted to represent the compressive strength of confined RPC to distinguish from f_{co} for fully loaded specimens. The calculation method as the same as that for fully loaded specimens has been used, and then the Eq. (21) could be obtained

$$f'_{co} = f_c + k_2 p \qquad (21)$$

Where k_2 is the strength coefficient. p is the lateral restraint force from the steel tube by analyzing the stress mechanism of partially loaded specimens. The steel tube has yielded and will be in plastic range at the ultimate state, so the value of p could be regarded as the plastic limit solution of thin-walled tubes

$$p = \frac{2f_y}{\sqrt{3}} \ln\frac{r_1}{r_0} \qquad (22)$$

Combining with above three equations, the axial capacity N_u can be expressed as follows

$$N_u = [f_c + k_2 \frac{2f_y}{\sqrt{3}} \ln\frac{r_1}{r_0}]A_c \qquad (23)$$

Where k_2 is an undetermined coefficient. By using the nonlinear curve-fitting toolkit in Mathematica, the coefficient is determined to be $k_2 = 3.06$ based on the test data, with a mean R^2 value of 0.96. And thus, the ultimate capacity could be presented as

$$N_u = [f_c + 10.6 f_y \ln \frac{r_1}{r_0}] A_c \qquad (24)$$

5.3.3 Results comparison

The axial capacity of test specimens from the literatures (Zhang 2003, Lin *et al.* 2005, Feng 2008, Luo *et al.* 2014) and this test are evaluated using Eqs. (19) and (24). The calculated results N_{ua} are compared with the test date N_{ue} for specimens with two load conditions, as shown in Fig. 11. As can be seen, the error between the calculated and test results is more uniform and within the range of 10%. The mean and variance are 0.99 and 0.65% for fully loaded specimen, while 1.01 and 0.22% for partially loaded specimens. So it can be concluded that the proposed methods can achieve a high precision, thus providing some useful references for predicting axial capacity of this composite column.

6. Conclusions

Through the experiment on the behavior of RPC filled circular steel tube short columns under axial compression, the calculation methods of axial capacity for specimens with two load conditions are proposed, and some other conclusions are also drawn, as follows:

- The fully loaded specimens display drum-shaped failure when with large confinement coefficients and shear failure when with small coefficients. The partially loaded specimens display shear failure except the specimen BZ10.0-1 which shows drum-shaped failure. The axial load keeps increasing after the peak for specimens with thick steel tubes, while with no or a slight increase for specimens with relatively thin steel tubes as the displacement increases.

- The load conditions have great influence on the axial load behavior of composite columns. The buckling of the steel tube could be avoided at the ultimate state when only applied to RPC core, which enables the steel tube to provide more effective confinement, consequently improving the capacity and ductility of columns. Moreover, the load capacity of columns will be higher with larger steel tube thickness and compressive strength of RPC, and high brittleness of unconfined RPC would be changed to ductile failure of steel tube confined RPC.

- The ratio of transverse strain to longitudinal strain ($\varepsilon_{sh}/\varepsilon_{sv}$) is stable at 0.2-0.3 at firstly, and the ratio becomes larger after the steel tube has yielded, indicating that the lateral confinement is gradually improved with the increasing load. By examining the measured strains, it can be seen that the confinement effect is not that significant in the early stages of loading for the fully loaded specimens, while this effect is important through all load stages for the partially loaded specimens.

- The axial capacity of the composite specimen is higher than that of the sum of the load capacities of its individual constituents (steel tube and RPC), thus reflecting the beneficial effect of confinement. All the specimens have higher bearing capacity after their failure, and the ratio of residual capacity to ultimate capacity increases when the confinement coefficients becomes larger and the steel tube yields earlier.

- The working mechanism and force model of composite columns are analyzed, and based on the twin-shear unified strength theory, calculation methods of axial capacity for RPC filled steel tube columns with two load conditions are established. The theoretical results from the proposed formulas have been in well agreement with the experimental data.

Acknowledgments

References

Abdulkareem, O.M., Fraj, A.B., Bouasker, M. and Khelidj, A. (2018), "Mixture design and early age investigations of more sustainable UHPC", *Constr. Build. Mater.*, **163**(28), 235-246.

Abid, M., Hou, X.M., Zheng, W.Z. and Hussain, R.R. (2017), "High temperature and residual properties of reactive powder concrete - A review", *Constr. Build. Mater.*, **147**, 339-351.

Aslani, F., Uy, B., Zhong, T. and Mashiri, F. (2015), "Predicting the axial load capacity of high-strength concrete filled steel tubular columns", *Steel Compos. Struct., Int. J.*, **19**(4), 967-993.

Chen, J., Liu, X., Liu, H.W. and Zeng, L. (2018), "Axial compression of circular recycled concrete-filled steel tubular short columns reinforced by silica fume and steel fiber", *Steel Compos. Struct., Int. J.*, **27**(2), 193-200.

Choi, I.P., Chung, K.S. and Kim, C.S. (2017), "Experimental study on rectangular CFT columns with different steel grades and thicknesses", *J. Constr. Steel Res.*, **130**, 109-119.

Du, Y.S., Chen, Z.H., Zhang, C.Q. and Cao, X.C. (2017), "Research on axial bearing capacity of rectangular concrete-filled steel tubular columns based on artificial neural network", *Front. Comput. Sci.*, **11**(5), 863-873.

Evirgen, B., Tuncan, A. and Taskin, K. (2014), "Structural behavior of concrete filled steel tubular sections (CFT/CFST) under axial compression", *Thin Wall. Struct.*, **80**, 46-56.

Feng, J.W. (2008), "Study on mechanical behavior of reactive powder concrete filled steel tubular columns", Ph.D. Dissertation; Tsinghua University, Beijing, China. [In Chinese]

GB 175 (2007), Common Portland Cement; General Administration of Quality Supervision, Inspection and Quarantine of the People's Republic of China; Beijing, China.

GB/T 31387 (2015), Reactive Powder Concrete; General Administration of Quality Supervision, Inspection and Quarantine of the People's Republic of China; Beijing, China.

Guler, S., Copur, A. and Aydogan, M. (2013), "Axial capacity and ductility of circular UHPC-filled steel tube columns", *Mag. Concrete Res.*, **65**(15), 898-905.

Han, L.H. and An, Y.F. (2014), "Performance of concrete-encased CFST stub columns under axial compression", *Int. J. Concr. Struct. M.*, **93**, 62-76.

Hoang, A.L. and Fehling, E. (2017), "Influence of steel fiber content and aspect ratio on the uniaxial tensile and compressive behavior of ultra high performance concrete", *Constr. Build. Mater.*, **153**, 790-806.

Huang, F.Y., Yu, X.M. and Chen, B.C. (2012), "The structural performance of axially loaded CFST columns under various loading conditions", *Steel Compos. Struct.*, *Int. J.*, **13**(5), 451-471.

Huynh, L., Foster, S., Valipour, H. and Randall, R. (2015), "High strength and reactive powder concrete columns subjected to impact: Experimental investigation", *Constr. Build. Mater.*, **78**(1), 153-171.

Li, H. and Liu, G. (2016), "Tensile properties of hybrid fiber-reinforced reactive powder concrete after exposure to elevated temperatures", *Int. J. Concr. Struct. M.*, **10**(1), 29-37.

Liang, W., Dong, J.F. and Wang, Q.Y. (2018), "Axial compressive behavior of concrete-filled steel tube columns with stiffeners", *Steel Compos. Struct.*, *Int. J.*, **29**(2), 151-159.

Lin, Z.Y., Wu, Y.H. and Shen, Z.Y. (2005), "Research on behavior of RPC filled circular steel tube column subjected to axial compression", *J. Build. Struct.*, **26**(4), 52-57. [In Chinese]

Luo, H., Ji, W.Y., Yan, Z.G. and Li, W.W. (2014), "Research on influence of loading methods on compression behavior of reactive powder concrete filled steel tube stub columns under axial loads", *J. China. Railway. Soc.*, **36**(9), 105-110. [In Chinese]

Luo, H., Wang, W.W., Shen, L. and Wang, G.H. (2017), "Stress-strain model for reactive powder concrete confined by steel tube", *J. Eng. Sci. Technol. Rev.*, **10**(2), 122-131.

Min, Y., Zha, X.X., Ye, J.P. and Li, Y.T. (2013), "A unified formulation for circle and polygon concrete-filled steel tube columns under axial compression", *Eng. Struct.*, **49**(2), 1-10.

Sanchayan, S. and Foster, S.J. (2016), "High temperature behavior of hybrid steel-PVA fiber reinforced reactive powder concrete", *Mater. Struct.*, **49**(3), 769-782.

Shan, B., Lai, D.D., Xiao, Y. and Luo, X.B. (2018), "Experimental research on concrete-filled RPC tubes under axial compression load", *Eng. Struct.*, **155**(15), 358-370.

Shi, C.H., Cao, C.Y., Long, G.C. and Lei, M.F. (2017), "Mechanical property test and analytical method for reactive powder concrete columns under eccentric compression", *KSCE J. Civil Eng.*, **21**(4), 1307-1318.

Thomas, J. and Sandeep, T.N. (2018), "Experimental study on circular CFST short columns with intermittently welded stiffeners", *Steel Compos. Struct.*, *Int. J.*, **29**(5), 659-667.

Wang, Q.W., Wang, Z.W. and Tao, Y. (2017), "Experimental research on effect of mix ratio and curing system on the strength of reactive powder concrete", *J. Xi'an Univ. of Arch. Tech.*, **49**(3), 382-387. [In Chinese]

Yan, K., Xu, C. and Zhang, X. (2016), "Compressive behavior of steel fiber-reinforced reactive powder concrete at elevated temperatures", *Sci. Adv. Mater.*, **8**(7), 1454-1463.

Yiğiter, H., Aydın, S. and Yardımcı, M.Y. (2012), "Mechanical performance of low cement reactive powder concrete (LCRPC)", *Compos. Part B-Eng.*, **43** (8), 2907-2914.

Zhang, J. (2003), "Experimental investigation on behavior of reactive powder concrete filled steel stub columns", Ph. D. Dissertation; Fuzhou University, Fuzhou, China. [In Chinese]

Zheng, W.Z., Luo, B.F. and Wang, Y. (2015), "Stress-strain relationship of steel - fibre reinforced reactive powder concrete at elevated temperatures", *Mater. Struct.*, **48**, 2299-2314.

CC